



## A new lineage of crayfish-infecting Microsporidia: The *Cambaraspora floridanus* n. gen. n. sp. (Glugeida: Glugeidae) complex from Floridian freshwaters (USA)



Jamie Bojko<sup>a,b,c,d,\*</sup>, Donald C. Behringer<sup>c,d</sup>, Paul Moler<sup>e</sup>, Cheyenne E.L. Stratton<sup>d</sup>, Lindsey Reisinger<sup>d</sup>

<sup>a</sup> School of Health and Life Sciences, Teesside University, Middlesbrough, Tees Valley, TS1 3BA, UK

<sup>b</sup> National Horizons Centre of Excellence for Bioscience Industry, Teesside University, Darlington DL1 1HG, UK

<sup>c</sup> Emerging Pathogens Institute, University of Florida, Gainesville, FL 32611, USA

<sup>d</sup> Fisheries and Aquatic Sciences, University of Florida, Gainesville, FL 32653, USA

<sup>e</sup> Florida Fish and Wildlife Conservation Commission, Gainesville, FL 32601, USA

### ARTICLE INFO

#### Keywords:

Microsporidia

Crayfish

Opisthosporidia

Pathogen

Parasite

Disease ecology

### ABSTRACT

Crayfish are a vital ecological asset in their native range but can be highly damaging as invasive species. Knowledge of their diseases, including high levels of research on *Aphanomyces astaci* (crayfish plague), show that disease plays a vital role during crayfish invasions. Microsporidian diseases in crayfish are less studied but are thought to have important links to crayfish health and invasion dynamics.

In this study we provide a systematic description of a novel microsporidian parasite from the Floridian crayfish, *Procambarus paeninsulanus*, with additional genetic identification from related Microsporidia from *Procambarus fallax*, *Cambarellus shufeldtii* and *Cambarellus blacki*. This novel microsporidium from *P. paeninsulanus* is described in a new genus, *Cambaraspora*, and species, *Cambaraspora floridanus*, and represents a novel member of the Clade V Microsporidia within the Glugeidae. The parasite develops in the muscle tissue of *P. paeninsulanus*, within a sporophorous vesicle, and produces a spore with 19–21 turns of the polar filament measuring  $6.136 \pm 0.84 \mu\text{m}$  in length and  $2.12 \pm 0.23 \mu\text{m}$  in width. The muscle-infecting nature of the parasite suggests that it is horizontally transmitted.

Genetic data for the 18S of the parasite from all hosts confirms its assignment to Clade V and reveal it to be a relative of multiple fish-infecting parasites. It shows closest genetic relationship to *Glugea plecoglossi*, but branches alongside multiple microsporidia from fish, crustaceans and eDNA isolates.

The information presented here suggests that this novel parasite may have the potential to infect piscine hosts and is a likely mortality driver in the *P. paeninsulanus* population. Its potential as a control agent or wildlife disease invasion threat is explored, as well as the placement of this novel microsporidium within the Glugeidae.

### 1. Introduction

The Microsporidia are a group of spore-forming, obligate, intracellular parasites that have been found to infect a high diversity of host taxa (Karpov et al., 2014; Vossbrinck et al., 2014). Microsporidian systematics currently revolve around five taxonomic clades, informed by SSU ribosomal gene sequence data (Vossbrinck et al., 2014). Clades I and III represent the Aquasporidia; Clades II and IV represent the Terresporidia; and Clade V represents the Marinospordia, a group of vertically or horizontally transmissible microsporidia that primarily target the muscle, gut, and/or gonad tissues of fish or invertebrates,

with one example (*Trachipleistophora hominis*) known to infect humans (Vossbrinck et al., 2014).

Clade V supports multiple microsporidian families, including the Pleistophoridae (Doflein, 1901), Myosporidae (Stentiford et al., 2010), Spragueidae (Weissenberg, 1976), Tetramicridae (Matthews and Matthews, 1980), and Glugeidae (Thélohan, 1895). The genera *Dicyocoela* (Bacela-Spychalska et al., 2018) and *Myosporidium* (Baquero et al., 2005) require formal systematic placement into a family supported by Clade V but are phylogenetically supported within this group. Many of the Clade V Microsporidia infect aquatic species, and a high diversity infect piscine and crustacean hosts (Stentiford et al., 2013).

\* Corresponding author.

E-mail address: [J.Bojko@tees.ac.uk](mailto:J.Bojko@tees.ac.uk) (J. Bojko).

Infection by these microsporidia causes issues for aquaculture and fisheries, often resulting in mortality of the host and posing potential risk as a source of human disease (*T. hominis*) (Cheney et al., 2000; Stentiford et al., 2016).

The Glugeidae family supports multiple genera within Clade V, including *Heterosporis*, *Loma*, *Ichthyosporidium*, *Pseudoloma*, and *Glugea* (Al Quraishi et al., 2019), all of which infect piscine hosts. Infection by members of this group often result in mortality of the fish host and can be the cause of xenomol growths, which are visually unsightly for fishing industries and retail (Al Quraishi et al., 2019). To date, no members of this group have been formally described from crustaceans.

Here, we describe a new genus and species of Microsporidia within the Glugeidae (Glugeida). Using PCR, additional isolates were found in *Procambarus fallax*, *Cambarellus schufeldtii* and *Cambarellus blacki*, revealing a genetically similar complex of isolates. The systematics of this new genus and species are based on genetic, phylogenetic, developmental, ultrastructural, and pathological data. The presence of this novel parasite in Florida freshwater systems, its crayfish host, and its taxonomic relation to the Glugeidae, are explored.

## 2. Materials and methods

### 2.1. Crayfish locality and collection

All crayfish were collected in the state of Florida, USA. *Procambarus paeninsulanus* (n = 4) were collected from the Big Blue Spring area (N30.32742, W-83.98494) of the Wacissa River system, Jefferson County, on the 29th of March 2019. *Procambarus fallax* (n = 3) were collected from Rodman Reservoir in Putnam County (N29.5424, W-81.8372 and N29.5423, W-81.7520) on the 23rd of April 2019. *Cambarellus blacki* (n = 1) exhibiting gross pathology was collected from the Escambia River floodplain (N30.9557, W-87.2191) on the 15th of April 2019. *Cambarellus shufeldtii* (n = 1) was collected from the Escambia River Floodplain, N30.7841, W-87.3179 on the 20th of March 2019.

*Procambarus paeninsulanus* and *C. blacki* were held in river water from the location at room temperature for 2 d before being delivered to the Aquatic Pathobiology Building at the University of Florida, Gainesville. Two of the four *P. paeninsulanus* exhibited “cotton-tail disease”, suggesting microsporidian infection. Individuals were dissected to remove muscle, heart, hepatopancreas, gut, gonad, gill, antennal gland, cuticle, nerve, and eye tissue for histology. In addition, muscle, hepatopancreas, and gill tissues were fixed in 2.5% glutaraldehyde in 0.1% sodium cacodylate buffer for transmission electron microscopy (TEM) and in 99% molecular grade ethanol for molecular diagnostics. *Cambarellus shufeldtii* was held in captivity until death in July 2019 after developing microsporidiosis in the laboratory. It was subsequently fixed whole in ethanol for DNA extraction.

To gain an idea of microsporidian prevalence, an additional 36 *P. fallax* were collected from the Rodman Reservoir (24th May 2019) and 67 *P. paeninsulanus* were collected from the Wacissa River (17th September 2019) and a piece of muscle tissue from the abdomen of each individual was fixed in 96% molecular grade ethanol.

### 2.2. Histopathology

Crayfish tissues were initially fixed in Davidson's freshwater solution (tap water, ethanol, formaldehyde, acetic acid) for 48 h before immersing in 70% ethanol. Ethanol-fixed tissues were then infiltrated with paraffin wax after further dehydration and xylene exchange. Wax-infiltrated tissues were embedded into a wax block and sectioned using a microtome to produce 3–4 μm thick sections. Each section was mounted onto a glass slide, dewaxed, dehydrated and stained with haematoxylin and alcoholic eosin. Finally, slides were cover-slipped. Histological processing was conducted by Histology Tech Services Inc. ([www.histologytechservices.com](http://www.histologytechservices.com)). Slides were read using a Leica light

microscope and images captured using an integrated Leica camera system.

### 2.3. Transmission electron microscopy

Infected muscle tissue from *P. paeninsulanus* was processed from 2.5% glutaraldehyde in 0.1% sodium cacodylate buffer into 4% glutaraldehyde with 2.5% paraformaldehyde in 0.1M sodium cacodylate pH 7.24. Fixed tissue was processed with the aid of a Pelco BioWave Pro laboratory microwave (Ted Pella, Redding, CA, USA). Samples were washed in 0.1M sodium cacodylate, pH 7.24, post fixed with buffered 2% OsO<sub>4</sub>, water washed and dehydrated in a graded ethanol and acetone series (25% through 100% with 5% increments followed by 100% acetone). Dehydrated samples were infiltrated with ARALDITE/Embed (Electron Microscopy Sciences (EMS), Hatfield, PA) and Z6040 embedding primer (EMS, Hatfield, PA) in increments of 3:1, 1:1, 1:3 anhydrous acetone:ARALDITE/Embed followed by 100% ARALDITE/Embed. Semi-thick sections (500 nm) were stained with toluidine blue. Ultra-thin sections were collected on carbon coated Formvar 100 mesh grid (EMS, Hatfield, PA) post-stained with 2% aqueous uranyl acetate [UO<sub>2</sub>(CH<sub>3</sub>COO)<sub>2</sub>] and lead citrate (C<sub>12</sub>H<sub>10</sub>O<sub>14</sub>Pb<sub>3</sub>) (EMS, Hatfield, PA). Sections were examined with a FEI Tecnai G2 Spirit Twin TEM (FEI Corp., Hillsboro, OR) and digital images were acquired with a Gatan UltraScan 2 k × 2 k camera and Digital Micrograph software (Gatan Inc., Pleasanton, CA).

### 2.4. Molecular diagnostics

DNA was extracted from up to 5 mg of microsporidian-infected muscle tissue from the abdomen of each individual using a quick-DNA extraction kit ([www.zymoresearch.com](http://www.zymoresearch.com)) according to manufacturer's protocol. The genomic DNA from the host and microsporidium was used in a Promega ‘Flexi-Taq’ PCR (50 μl reaction volume) consisting of 1 μM forward primer MF1 (5'-CCGGAGAGGGAGCCTGAGA-3'), 1 μM reverse primer MR1 (5'-GACGGGGGTGTGTACAAA-3') (Tourtip et al., 2009), 1 mM dNTPs, 0.25 μl of Promega Taq polymerase and 2.5 mM MgCl<sub>2</sub>. In addition, the same mixture was used with the V1F (5'-CAC CAGGTTGATTCTGCCTGAC-3') and Mc3r (5'-GATAACGACGGGGGT GTGTACAA-3') primers to gather additional sequence data (Baker et al., 1994; Ovcharenko et al., 2010). The thermocycler conditions for both reactions consisted of an initial denaturation at 94 °C (4 min) followed by 36 cycles of 94–55–72 °C, with each temperature held for 1 min, and a final extension period at 72 °C for 7 min. The resulting amplicons were visualised using gel electrophoresis on a 1.5% agarose gel and amplifications of both the host (~1200 bp) and parasite (~900 bp) were present. The microsporidian bands were excised from the gel and sent for forward and reverse sequencing using Eurofins Genomics ([www.eurofinsgenomics.com](http://www.eurofinsgenomics.com)). This resulted in microsporidian sequence data of the following sizes from the following hosts: *P. paeninsulanus*, 888 bp (NCBI accession: MT006315); *C. schufeldtii*, 1204 bp (MT006313); *C. blacki*, 1215 bp (MT006314); *P. fallax*, 935 bp (MT006316).

Additional PCR amplifications were conducted on 36 *P. fallax* and 67 *P. paeninsulanus* tissues to determine microsporidian prevalence. We used the V1f/Mc3r primer set as described above. Resulting amplicons were sequenced and those with high similarity were included in the statistical analyses.

### 2.5. Phylogenetics and genetic comparisons

The 888 bp sequence of the 18S gene from the novel microsporidian infecting *P. paeninsulanus* was phylogenetically evaluated and compared with 132 other microsporidian 18S genes, plus four isolates from ‘Clade IV’ of the Microsporidia (*Enterocytozoon hepatopenaei*, *Nucleospora cyclopteri*, *Vittaforma* sp., and *Parahepatospora carcinii*) as an out group. The 140 isolates were selected for comparison as either

representative genera within 'Clade V' of the Microsporidia, were isolated from crayfish, or were within 16% similarity to the sequence of the novel microsporidian. The sequences were aligned using Geneious (v.10.0.2) MAFFT protocol to result in 1252 positions. This alignment was analysed for the best fitting model using IQtree webserver (Trifinopoulos et al., 2016) and resulted in the GTR + F + G4 model choice according to BIC. The final tree was developed using a Maximum Likelihood process with 1000 bootstrap replicates of the sequence data and had a log likelihood of  $-21145.137$ .

A distance matrix was used to compare the four isolates of the new species and *Microsporidium cypselurus* (AJ300706) as a comparison to a related isolate. This was conducted in the Sequence Demarcation Tool (v1.2) (Muhire et al., 2014).

## 2.6. Statistical analysis

The animals collected from the Rodman and Wacissa river systems were measured for size (continuous data) and sex (factorial data) in addition to the application of a diagnostic PCR (V1F/Mc3r primers) to test for the presence of microsporidia (binomial data: presence/absence). The continuous data were normally distributed for the Rodman animals (Shapiro,  $w = 0.97$ ,  $p = 0.57$ ) and the Wacissa animals (Shapiro,  $w = 0.99$ ,  $p = 0.83$ ). Comparisons between the carapace length data and binomial infection data were conducted using a Welch two sample *t*-test. Sex and binomial infection data were compared using a fisher exact test.

## 3. Results

### 3.1. Gross pathology, histopathology and prevalence

Infected *P. paeninsulanus* muscle tissue was white and visible through the ventral cuticle of the abdomen, relative to the translucent muscle tissue observed in uninfected conspecifics (Fig. 1a–b). Histological screening of the two infected specimens and the two uninfected specimens revealed that microsporidian spores were only present in the two animals exhibiting gross pathology of infection. The muscle tissue of infected animals revealed multiple packets of spores (containing up to 32 individual spores) at different developmental stages that appeared to primarily situate in the sarcolemma of host muscle fibres, including skeletal muscle, heart muscle and smooth muscle (Fig. 2a). As the parasite developed through various life stages, these packets (presumably sporophorous vesicles) enlarged to accommodate multiple life stages, including the final infective spore (Fig. 2b and c). Release of spores through ruptured muscle fibres was also noted (Fig. 2d). Smaller

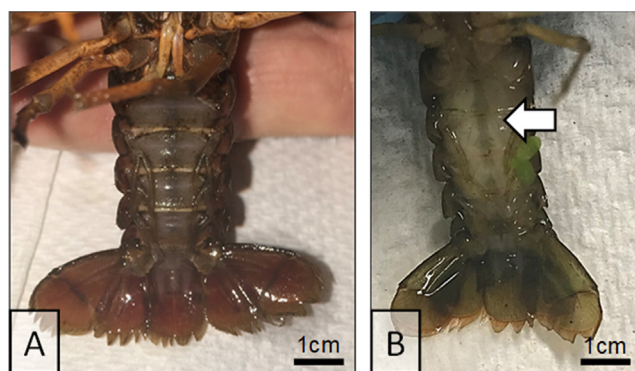


**Fig. 1.** *Procambarus paeninsulanus* uninfected (A) and infected (B) with *Cambaraspora floridanus* n. sp. collected from the Wacissa River, Florida. (A) muscle tissue visible through the thin ventral cuticle of the animal is translucent; (B) muscle tissue exhibiting infection is white (white arrow). Muscle at the rear of the animal's abdomen remains clear of visible infection and is translucent.

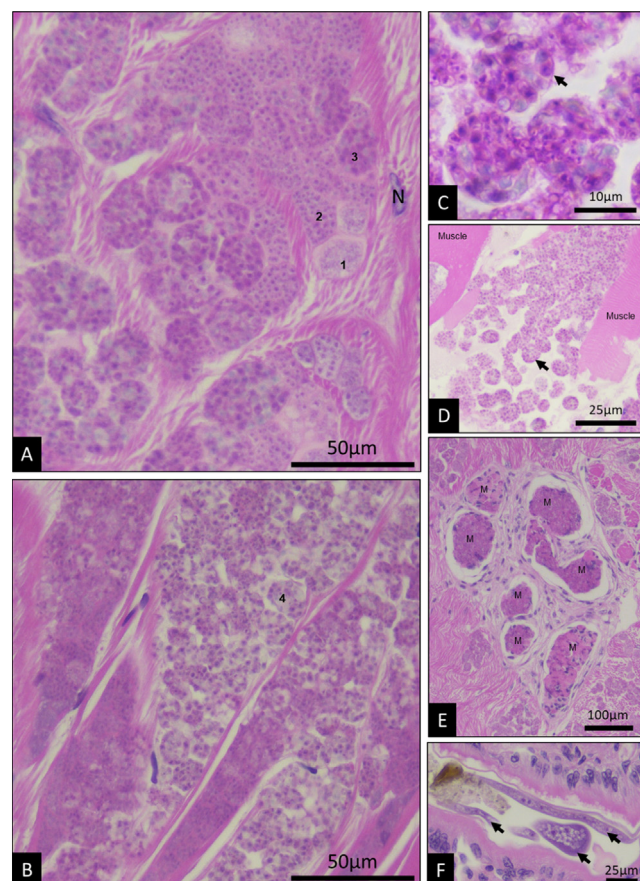


**Fig. 2.** Histological images of infected crayfish tissues. (A) Muscle tissue (nucleus = N) is the seat of infection for the microsporidian parasite, which goes through multiple developmental stages, including early stage, mid-stage and late-stage. (B) Muscle tissue exhibiting late-stage infection revealed multiple packets of mature spores (4). (C) A 1000 $\times$  magnified image of the mature packets of spores (black arrow). (D) Mature spore packets (black arrow) being released into a haemal sinus after rupture of the muscle tissue. (E) In some tissues, the infection resulted in the production of granulomas. (F) Gregarine parasites (black arrow) in the gut lumen.

populations of spores were observed systemically in the animal, in the haemolymph around the gills, gonad, and hepatopancreas, but did not appear to result in infection of these organs. Immune responses in the form of melanisation, presumably towards the microsporidian parasite, were noticed in the antennal gland and muscle tissues (Fig. 2e).

Prevalence of infection in *P. fallax* collected from the Rodman site was 13.8% (5/36) and was 16.4% (11/67) in *P. paeninsulanus* from the Wacissa. Size range in the *P. fallax* population was 10.0–37.6 mm and the sex ratio was 5:31 (M:F). Smaller *P. fallax* were significantly associated with infection (*t*-test,  $t = 2.64$ ,  $df = 5$ ,  $p \leq 0.05$ ). Four females and one male were infected; however, our data suggest this is not a significant difference for the population size sampled (Fisher test, ratio = 1.66,  $p = 0.55$ ). A size range of 11–38.5 mm was observed in the *P. paeninsulanus* population, with a sex ratio of 28:39 (M:F). Smaller *P. paeninsulanus* were significantly associated with the infection (*t*-test,  $t = 2.34$ ,  $df = 13.14$ ,  $p \leq 0.05$ ). Six females and four males were infected; however, neither sex showed a significantly higher relative prevalence of infection (Fisher test, ratio = 0.92,  $p = 1.00$ ). In addition to infection by the microsporidian parasite, apicomplexan protists (gregarines) were present in the gut lumen of a single *P. paeninsulanus* (Fig. 2f).

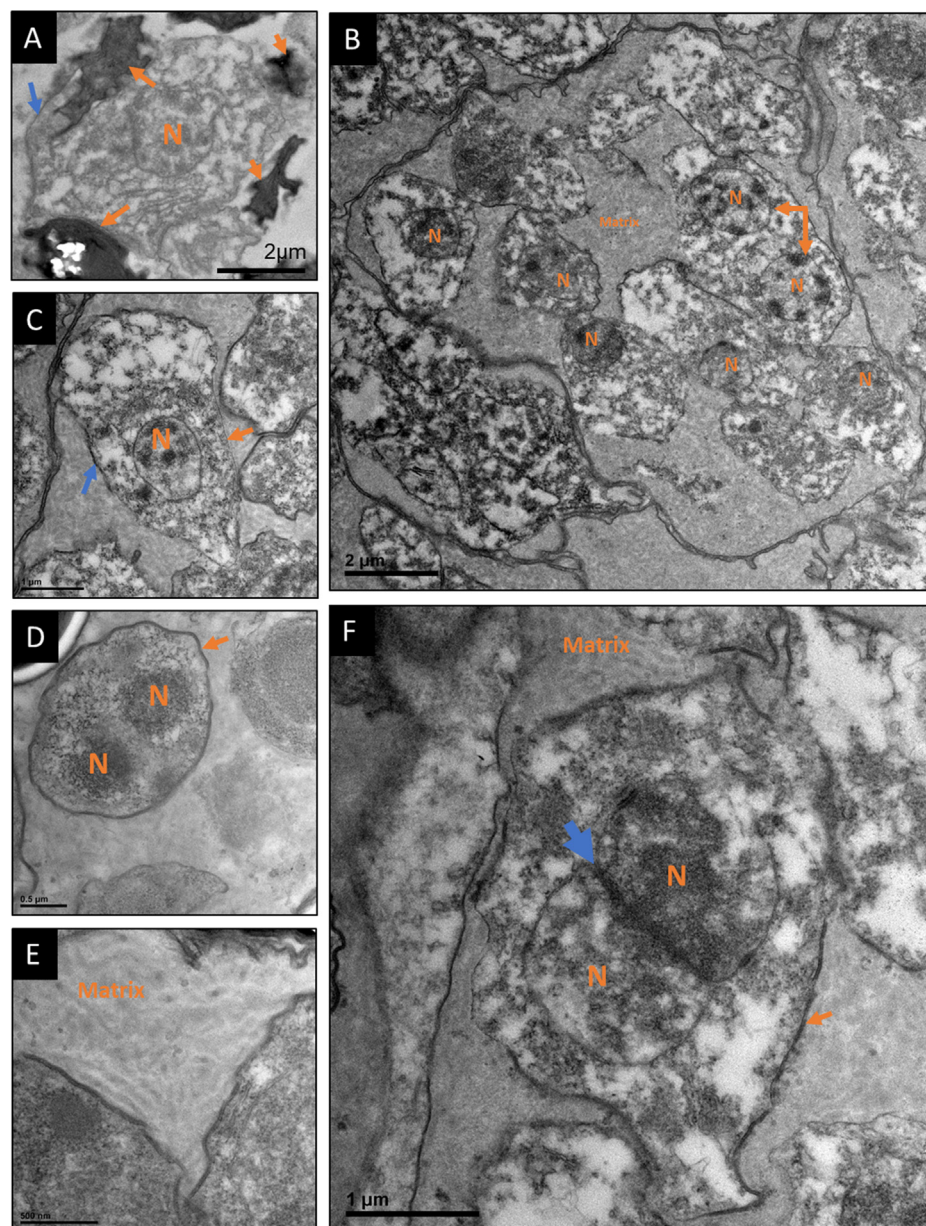


**Fig. 3.** Early development of *Cambaraspis floridanus* n. gen. n. sp. (Merogony). (A) A putative monokaryotic meront ( $n = \text{nucleus}$ ) with clear cytoplasm and thin cell wall (blue arrow). Unknown, electron dense, bodies appear around the earliest life stages (orange arrow). (B) A lower magnification image of merogony occurring in a sporophorous vesicle. Early nuclei (N) have divided (arrows) in the early meront, which is electron lucent and in contact with the sporophorous matrix ("Matrix"). No diplokaryotic meronts are present at this stage. (C) A higher magnification image of a single uninuclear (N) sporophorous meront, whose cell wall is beginning to thicken (blue and orange arrows). (D) Division of the nucleus to become a diplokaryotic sporophorous meront, noting the thickening of the membrane as the stage develops towards sporogony. (E) A high magnification image of the sporophorous matrix of interwoven proteins. (F) The diplokaryotic meront (2N) with bound nuclei (blue arrow), dark cell wall (orange arrow). (For interpretation of the references to colour in this figure legend, the reader is referred to the web version of this article.)

### 3.2. Ultrastructure and intracellular microsporidian development cycle

TEM of infected muscle tissue provided ultrastructural and developmental cycle data for this novel microsporidian species. The developmental cycle of the parasite begins with the diplokaryotic infective spore injecting its contents into the sub sarcolemmal space of the host muscle fibre (this may begin with the smooth muscle surrounding the gut), which is the primary site of infection (Fig. 2). The cell wall of the diplokaryotic meront appeared to thicken to become the membrane of the sporophorous vesicle (Fig. 3a), which filled with a protein rich matrix as the nuclei divided and separated within the expanding sporophorous vesicle (Fig. 3b). The electron lucent cytoplasm of the meront was observed to dissipate as the original nuclei from the diplokaryotic meront separate and divide (Fig. 3b). Each nucleus attained a cell membrane and individual cytoplasm within the sporophorous vesicle; the cytoplasm was electron lucent and became darker, as did the membrane, as it thickened (Fig. 3c-d). The matrix surrounding each meront became a light interwoven web of proteins (Fig. 3e). The nucleus of each meront then divided to form a diplokaryotic meront, with an increasingly thickened cell wall (Fig. 3f). Up to 24 individual

developing microsporidian cells were noted in histological and TEM cross-section, suggesting that this species develops in sets of 32.

Sporogony appeared to occur at different times for each of the microsporidian forms within the sporophorous vesicle, with some at late stage (pre-infective spore), mid-stage (mid-sporogony developmental stage) and early stage (late merogony) of development (Fig. 4). Early sporogonic forms were noted based on the dark cell wall and appearance of early developing spore organelles (Fig. 4a). The nucleus was relatively large at this stage and decreased in size throughout sporogony. The cell wall thickened throughout sporogony and the development of a bi-laminar polaroplast was noted to develop before other spore-specific organelles (Fig. 4b-c). The spore wall continued to become electron dense but develops a dark exosporous layer and dark cell membrane, relative to the thin endospore (Fig. 4d). Golgi and rough endoplasmic reticuli were abundant at this stage of development and appeared to develop from an amorphous mass at the periphery of the sporogonic cell (Fig. 4d). The endospore next began to become electron lucent as it thickened, and an early polar filament developed (Fig. 4e). At this stage the polar vacuole was also partitioned and visible in TEM section (Fig. 4f).

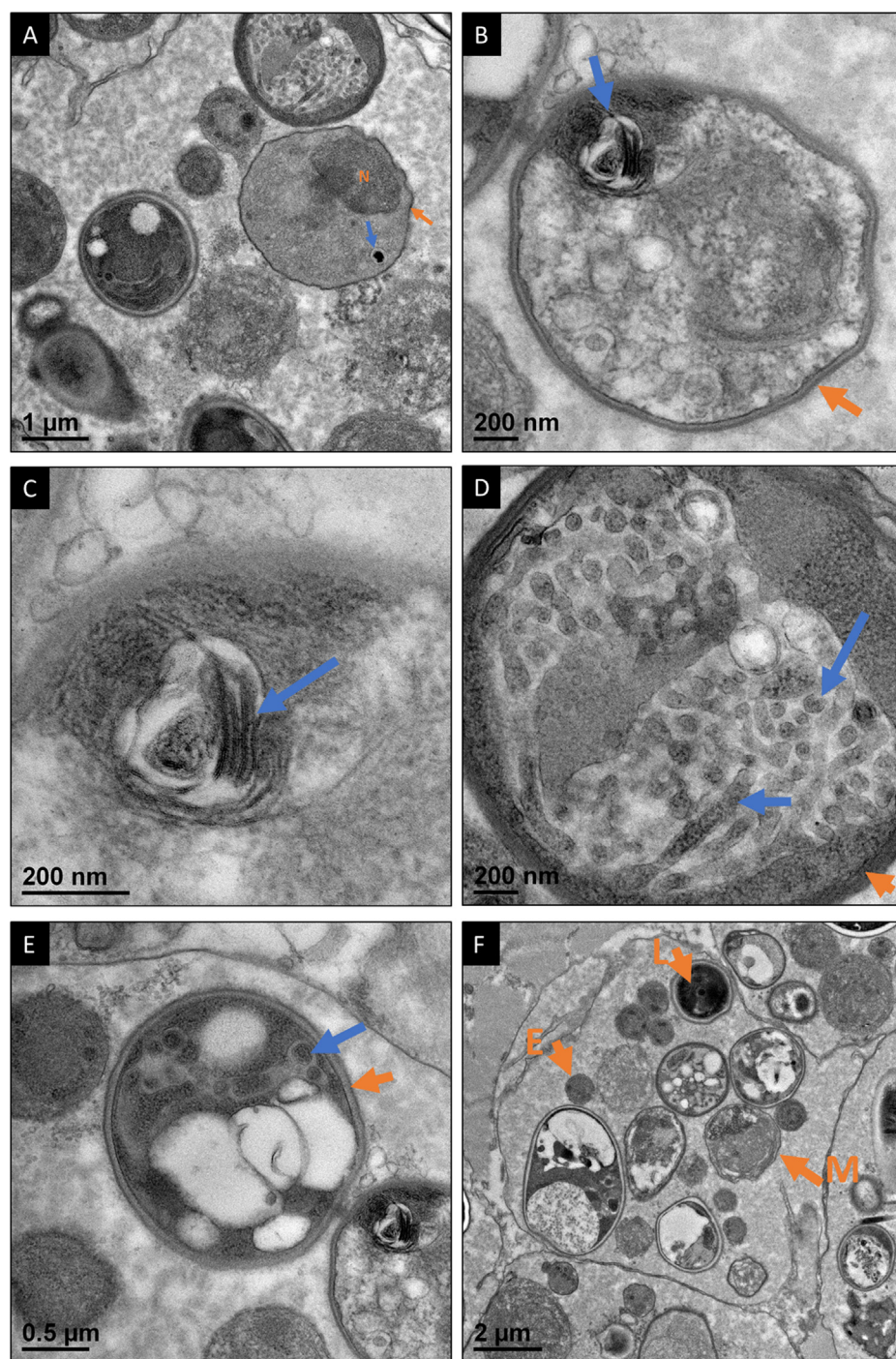


**Fig. 4.** Microsporidian sporogony of *Cambaraspis florianus* n. gen. n. sp. (A) Multiple developing microsporidians, at different stages of development, are present in a single sporophorous vesicle. Once merogony is complete, the cytoplasm and nuclei (N) darken and the cell begins to develop organelles (blue arrow) and a thick, electron dense cell wall. (B) The sporoblast stage includes development of the polaroplast (blue arrow) and the endospore and exospore can be differentiated (orange arrow). (C) A higher magnification image of the developing polaroplast (blue arrow) at the periphery of the developing spore. (D) The golgi and rough endoplasmic reticulum (blue arrows) appear to over-proliferate in the spore, displacing the darkening cytoplasm. The cell wall continues to thicken and darken (orange arrow). (E) The endospore begins to lighten, where the cell membrane and exospore remain dark (orange arrow). The polar filament begins to form (blue arrow). (F) As multiple sporoblasts begin to reach the mature spore developmental stage, other cells continue to develop at different rates. This image identifies a merogonal stage (E), an early sporoblast stage (M) and dark, late stage sporoblast (L) spore in a single sporophorous vesicle. (For interpretation of the references to colour in this figure legend, the reader is referred to the web version of this article.)

The final stages of sporogony included an elongation of the spore into a cucumiform shape and arrangement of the irregular polar filament (19–21 coils) at the periphery of the cell, against the spore wall (Fig. 5a–b). Prior to final maturity, the microsporidian spore included all mature organelles with a lighter staining cytoplasm (Fig. 5c) relative to the final spore (Fig. 6a). The mature spore included a bi-laminar polaroplast, anchoring disk, coiled polar filament, two nuclei, and a polar vacuole. The mature spore was  $6.136 \pm 0.84 \mu\text{m}$  ( $n = 12$ , SD) in length and  $2.12 \pm 0.23 \mu\text{m}$  ( $n = 12$ , SD) in width. The spore wall was  $150.83 \pm 22.69 \text{ nm}$  ( $n = 10$ , SD) in thickness around the majority of the spore but was thinner [ $91.09 \pm 23.19 \text{ nm}$  ( $n = 10$ , SD)] at the anchoring disk (Fig. 6b). The polar vacuole did not infiltrate well enough to provide an image of the final mature spore in full cross-section.

Some life stages of the parasite were rarely observed, often at the

earliest levels of merogony in typical microsporidian development (Fig. 6c). These cells were electron dense and included a thin and irregularly shaped cell wall and possible remnants of polar filament. Some were in elongated and irregular shapes (Fig. 6c). Their position within the lifecycle is currently unknown. A graphical representation of the intracellular life cycle of the newly identified microsporidian parasite is provided in Fig. 7.

### 3.3. Genetic similarity and phylogenetic placement of the novel isolates

The 18S rRNA genes from the complex of isolates were compared using a distance matrix, and we determined that all isolates were 98.4–99.8% similar (Fig. 8). The isolates from *Procambarus* hosts showed higher similarity to one another (99.8%) relative to the

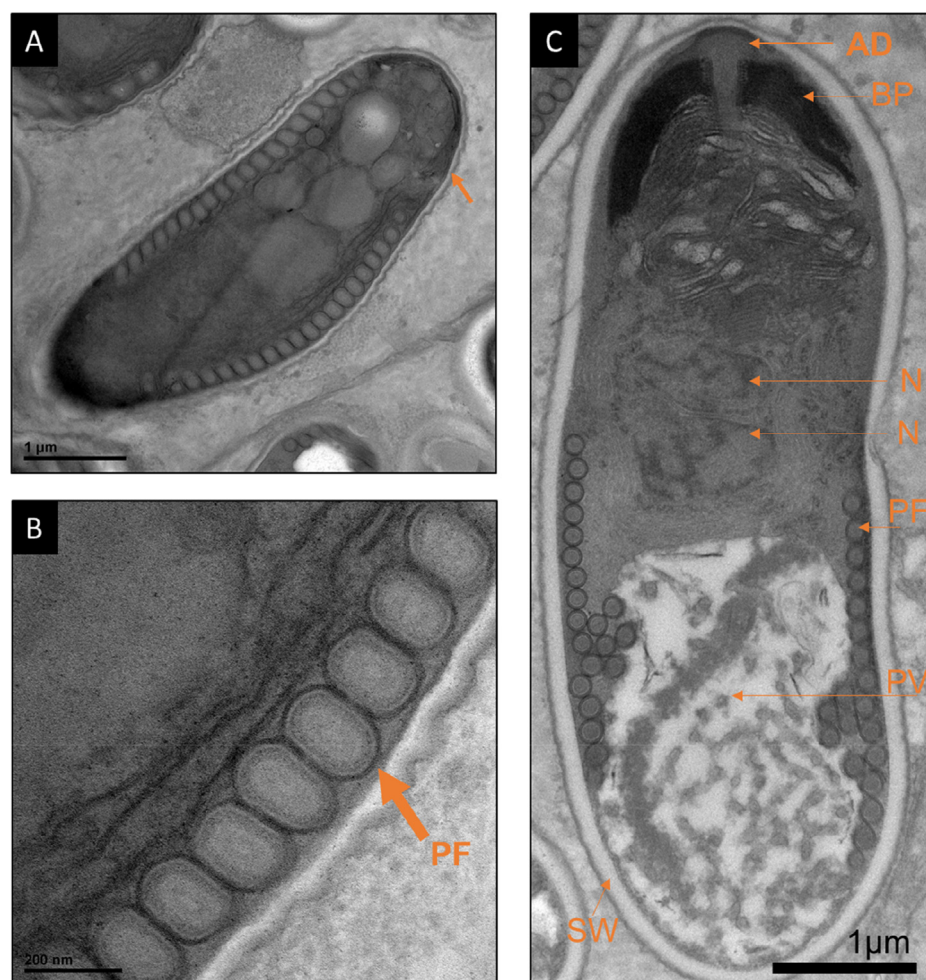


**Fig. 5.** Late sporoblast anatomy. (A) Prior to maturity, the sporoblast elongates, has an electron lucent endospore (orange arrow), and the polar filament arranges around the periphery of the spore. (B) The polar filament remains flexible and irregular. It includes rings of protein of variable electron density (PF). (C) The mature spore includes a thickened multi-layered spore wall (SW), polar vacuole (PV), anisofilar polar filament (PF) that tapers at the last two coils, diplokaryon (N), electron dense layer of a bi-layered polaroplast (BP) and anchoring disk (AD). (For interpretation of the references to colour in this figure legend, the reader is referred to the web version of this article.)

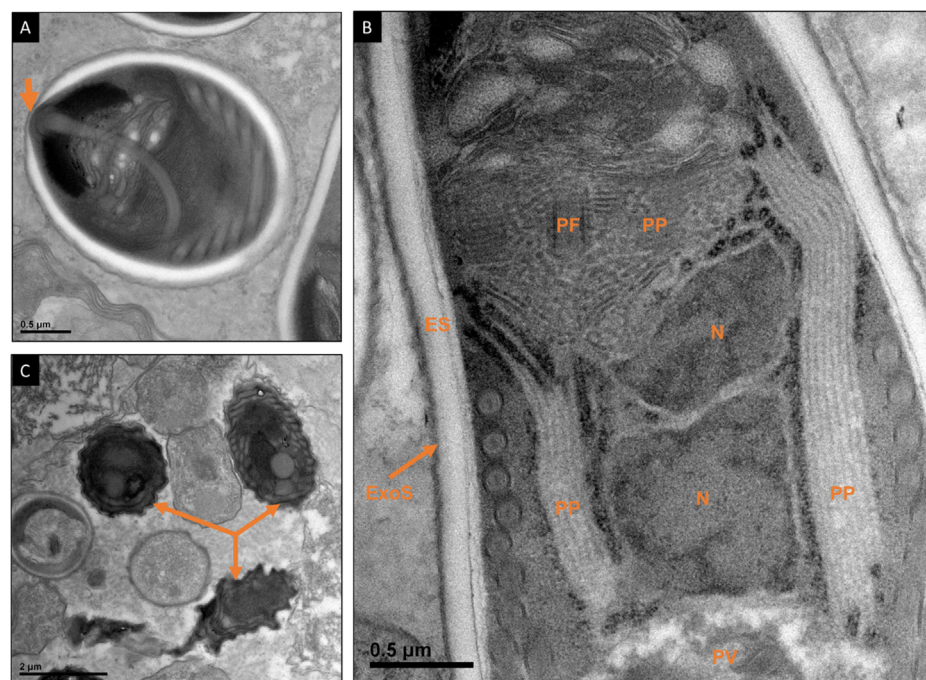


**Fig. 6.** Spore ultrastructure. (A) The anchoring disk and polar filament sit at the spore wall, which is thinner than the rest of the spore (orange arrow). (B) The ultrastructure of the diplokaryotic spore (N), a polar vacuole (PV), and a bi-laminar polaroplast (PP), which extends below the nuclei to the PV. The endospore (ES) remains electron lucent and the exospore (ExoS) is dark and lacks obvious features. A glancing section of the polar filament (PF) is present in section through the PP. (C) Electron dense sporoblasts (orange arrows) are present in multiple sporophorous vesicles. (For interpretation of the references to colour in this figure legend, the reader is referred to the web version of this article.)

similarity shared by the isolates from *Cambarellus* hosts (99.4%) (Fig. 8).

Phylogenetics conducted for the new *P. paeninsularus* isolate

included sequence isolates from all four crayfish hosts and identified the complex as part of the 'Clade V' Microsporidia, according to the updated clade definitions by Vossbrinck et al. (2014). The 888 bp

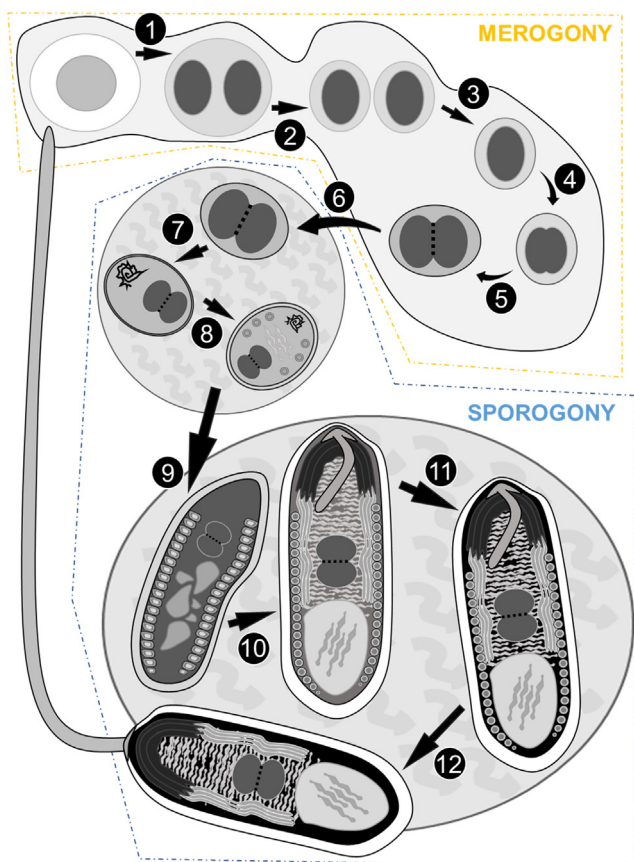


**Fig. 7.** A graphic representation of the developmental cycle of *Cambaraspore florianus* n. gen. sp. including merogony and sporogony. (1) One of two uninuclear meronts begin the developmental cycle (Fig. 3A). (2) The nuclei divide (Fig. 3B). (3) The nuclei continue to divide to produce 32 developing spores (Fig. 3B). (4) The nuclei divide to produce a diplokaryotic sporont (Fig. 3D, F) (5). (6) Between stages 5 and 7, the matrix of the sporophorous vesicle becomes increasingly proteinaceous (Fig. 3E). (7–8) Sporogony begins and the developing sporoblast produces a thicker wall and organelles (Fig. 4A–F). (9–11) the sporoblast progresses to develop organelles within the sporophorous vesicle and eventually produces a darkened cytoplasm and electron lucent wall, signifying maturity (Figs. 5 and 6). (12) The mature microsporidian spore exits the vesicle to infect a new cell/host, possibly through the breakdown/necrosis of host tissues.

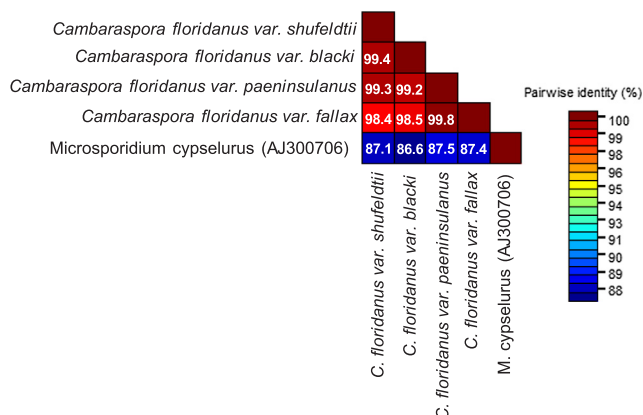


**Fig. 8.** A distance matrix comparison of the *Cambaraspore* complex using isolates from *Procambarus paeninsulanus*, *Procambarus fallax*, *Cambarellus shufeldtii* and *Cambarellus blacki*. Additional comparison is made to *Microsporidium cypselurus* (unofficial description), which represents a closely related isolate.

sequence from *P. paeninsulanus* showed highest NCBI BLASTn score with *Glugea plecoglossi* (KY882286: 100% cov.; 89.30% sim.; e-value: 0.0) isolated from *Sardina pilchardus* in the Atlantic, and highest similarity with a different isolate of the same species (AJ295326: 88% cov.; 89.39% sim.; e-value: 0.0) isolated from *Plecoglossus altivelis* in Japan. The new isolate showed relative levels of similarity to *T. hominis* (AJ002605: 100% cov.; 86.33% sim.; e-value: 0.0).

The phylogeny placed the *P. paeninsulanus* isolate as a mid-branching member of the ‘Clade V’ Microsporidia (Glugeida: Glugeidae) and different from all previously described genera, including the genus *Glugea*, with a confidence of 99% (Fig. 9). Branching alongside it at 70% confidence was an uncharacterised microsporidian parasite in the holding genus “*Microsporidium*”, *Microsporidium cypselurus* (AJ300706: 86% cov.; 87.45% sim.; e-value: 0.0), isolated from flying fish (*Cypselurus pinnatibarbatus*) from Yakushima, Japan (Fig. 9). There were unidentified branching species below and above the branch containing the new isolate and *Microsporidium cypselurus*. The branch below contained *Microsporidium* sp. STF (AY140647: 100% cov.; 88.89% sim.; e-value: 0.0) isolated from *Salmo trutta fario*. The branch above contained two uncharacterised species, an uncultured eukaryote clone (GU823864: 100% cov.; 88.06 sim.; e-value: 0.0) from an anoxic water column sample, Cariaco Basin, Caribbean Sea; and “*Pleistophora* sp. PA” (AJ252958: 100% cov.; 87.40% sim.; e-value: 0.0) an uncharacterised microsporidium from *Penaeus aztecus* in the USA (Fig. 9).

The new *P. paeninsulanus* isolate shows little genetic similarity to other microsporidia identified from crayfish hosts, including *Ovipleistophora diplostomuri* recently reported from *Procambarus bivittatus*, which shares a similar pathology (Bojko et al., 2020; Table 1). The phylogeny presented herein identified all crayfish-infecting microsporidia with available SSU sequence data to be outside of Clade V, with the exception of the newly identified isolate, which is placed in the Glugidae (Fig. 9; Fig. 10). *Vittaforma* sp. PLDH3 (AM261754) was present in the Clade IV out group of Fig. 8 and *Vairimorpha* sp. from Clade I. *Bacillidium* sp. PLFB32 (AM261748) was not included in the phylogeny due to short sequence information; however, comparison with existing isolates suggest this microsporidian shows closest similarity to *Bacillidium vesiculoformis* (AJ581955: 76% cov.; 97.26% sim.; e-value = 0.0) from Clade III. *Microsporidium* sp. PLWB7A (AM261749) was not included in the phylogeny due to short sequence information; however, comparison with existing isolates suggests this microsporidian shows closest similarity to *Pseudonosema cristatellae* (AF484694: 86% cov.; 76.71% sim.; e-value:  $1 \times 10^{-89}$ ) from Clade I. Finally, *Thelohania* sp. that infect crayfish remain systematically pending in reference to their clade but branch alongside the *Vairimorpha* sp. (Fig. 10).

#### 4. Taxonomic summary

##### 4.1. Higher taxonomy

*Super-group:* Opisthokonta

*Super-Phylum:* Opisthosporidia Karpov et al. (2014)

*Phylum:* Microsporidia Balbiani (1882)

*Class:* Marinospordia “Clade V” Vossbrinck et al. (2014)

*Order:* Glugeida [Recently reported by Al Quraishi et al. (2019)]

(Original description unknown)

*Family:* Glugeida Thélohan (1895)

*Type genus:* *Glugea* Thélohan (1895)

*Other genetically similar genera:* *Heterosporis*, *Loma*, *Ichthyosporidium*, *Pseudololoma*

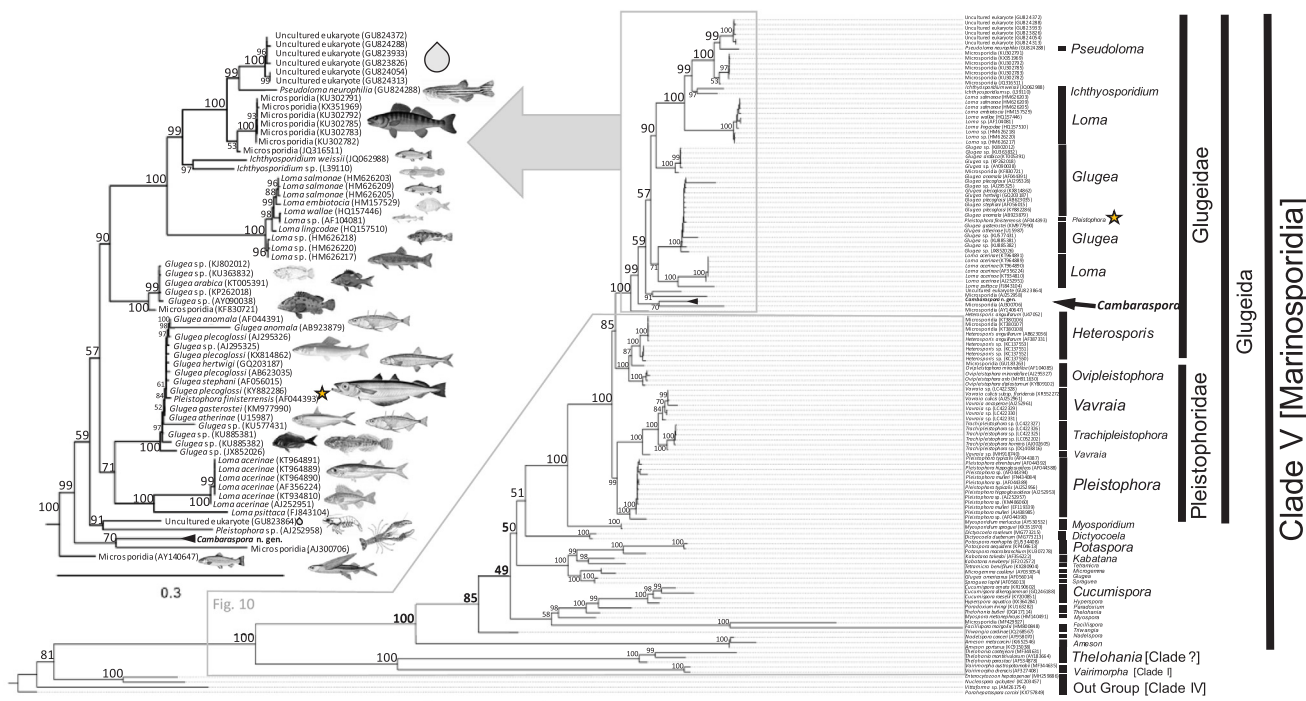


**Fig. 9.** A phylogenetic tree of all microsporidian isolates with > 84% similarity to *Cambaraspora floridanus* n. gen. n. sp. (bold; black arrow), and representatives of multiple Clade V genera and other Clades (I, III, IV) representing outgroups. A star highlights a *Pleistophora* isolate that is more likely a *Glugea* member. A more detailed section of the tree is highlighted, identifying multiple microsporidian hosts from which these isolates were obtained. Scales are presented for both the highlighted and complete phylogenetic trees (0.3 Units).

#### 4.2. Genus description for *Cambaraspora* n. gen. Bojko et al.

**Genus description:** Members of this genus infect the muscle tissue of aquatic crustacean hosts and undergo merogony and sporogony in a sporophorous vesicle. The spores are diplokaryotic and include 19–21 coils of the polar filament. The polaroplast is bi-laminar, with an electron dense upper layer and electron lucent lower layer. The spores are cucumiform in shape. Multiple developing life stages are evident in a single sporophorous vesicle. Genetic relatedness to the type species should be considered if placing a novel member into this genus.

**Type species:** *Cambaraspora floridanus* n. gen. n. sp. Bojko et al.

#### 4.3. Species description for *Cambaraspora floridanus* n. gen. n. sp. Bojko et al.

**Species description:** This species infects the muscle tissue of *Procambarus* sp. and *Cambarellus* sp. and undergoes merogony and sporogony in a sporophorous vesicle. The spores are diplokaryotic and include 19–21 coils of the polar filament. The polaroplast is bi-laminar, with an electron dense upper layer and electron lucent lower layer. The spores are cucumiform in shape and measure  $6.136 \pm 0.84 \mu\text{m}$  (SD) in

length and  $2.12 \pm 0.23 \mu\text{m}$  (SD) in width. Development of the polaroplast occurs first, followed by rough endoplasmic reticulum, polar filament, and polar vacuole. Multiple developing life stages are evident in a single sporophorous vesicle.

**Type host:** *Procambarus paeninsulanus*

**Type locality:** Wacissa River (N30.32742, W-83.98494), Jefferson County, Florida, USA.

**Site of infection:** This species infects the muscle tissue of the host.

**Etymology:** The genus is named for the two host genera (*Cambarellus* and *Procambarus*) in which this novel species was found to infect, and the species was named for the locality of the host and the parasite.

**Type material:** Original material is stored at the University of Florida, Behringer Laboratory.

## 5. Discussion

Microsporidian parasites are abundant in aquatic environments, and multiple species are known to infect crayfish (Longshaw, 2011). These hosts are often keystone ecosystem engineers in aquatic environments, and many have been identified as invasive and non-native species on a global scale (Gherardi et al., 2011). Members of the genus *Procambarus*

**Table 1**

Sequence similarity comparison of all crayfish-infecting microsporidian isolates relative to the 888 bp sequence from *Cambaraspora floridanus* n. gen. n. sp.

Isolate/Species	NCBI Accession	Host	Coverage	Similarity	E-value
<i>Thelohania contejeani</i>	MF344631	<i>Austropotamobius pallipes</i>	35%	72.67%	$1 \times 10^{-40}$
<i>Thelohania montivulorum</i>	AY183664	<i>Cherax destructor destructor</i>	40%	70.50%	$7 \times 10^{-37}$
<i>Thelohania parastaci</i>	AF294779	<i>Cherax destructor rotundus</i>	48%	69.49%	$5 \times 10^{-52}$
<i>Nosema austropotamobii</i>	MF344635	<i>Austropotamobius pallipes</i>	47%	72.71%	$2 \times 10^{-55}$
<i>Nosema cheracis</i>	AF327408	<i>Cherax destructor destructor</i>	46%	71.89%	$1 \times 10^{-52}$
<i>Bacillidium</i> sp. PLFB32	AM261748	<i>Pacifastacus leniusculus</i>	24%	72.16%	$8 \times 10^{-22}$
<i>Microsporidium</i> sp. PLWB7A	AM261749	<i>Pacifastacus leniusculus</i>	6%	87.50%	$4 \times 10^{-6}$
<i>Vittaforma</i> sp. PLDH3	AM261754	<i>Pacifastacus leniusculus</i>	37%	78.85%	$5 \times 10^{-22}$
<i>Ovipleistophora diplostomuri</i>	MN510506	<i>Procambarus bivittatus</i>	100%	87.79%	0.0

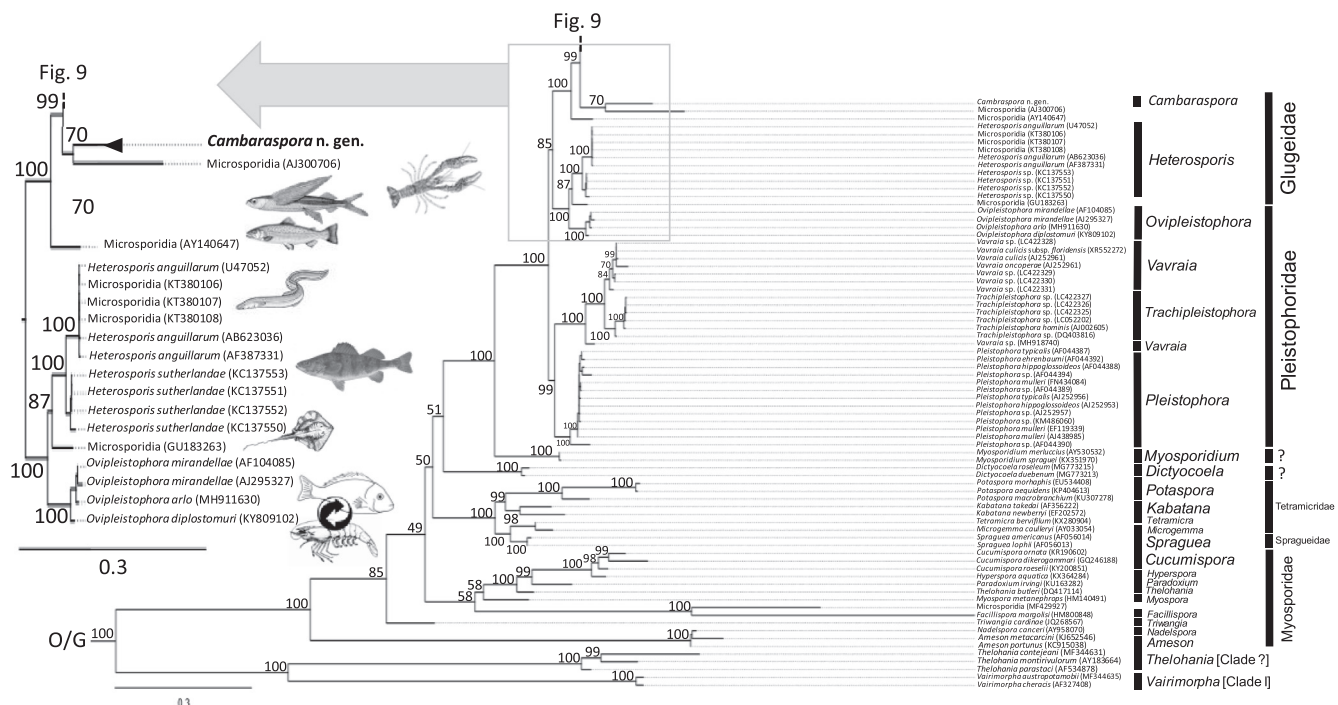


**Fig. 10.** A more detailed version of a portion of Fig. 8. This tree presents all the isolates that branch more basally to *Cambaraspora floridanus* n. gen. n. sp. (**bold**) within Clade V, highlighting the relevant taxonomic family of each genus. Images of representative hosts are present on the highlighted portion of the tree as well as those species that appear to be trophically transmissible between fish and crayfish. Scale bars are presented for both trees (0.3 Units).

are known to harbour multiple parasite groups (Longshaw, 2011); however, this study provides the first insight into a microsporidian pathogen of this genus. Some members of this genus are known to be prolific invaders and their microsporidian diseases might be viable biological control options. Alternatively, this group might initiate disease in other wildlife and may threaten native crayfish species.

### 5.1. Microsporidian diversity in crayfish

Microsporidian pathogens associated with crayfish have been found across the Microsporidia, in almost all clades, including taxa such as *Thelohania* sp. (Clade III), *Vittaforma* sp. (Clade IV), *Nosema* (= *Vairimorpha*) sp. (Clade I), *Vavraia parastacida* (Clade V), *Pleistophora soganderesi* (Clade V) and *Bacillidium* sp. (Clade III) (Moodie et al., 2003; Longshaw, 2011; Vossbrinck et al., 2014; Pretto et al., 2018). *Cambarasporea floridanus* n. gen. n. sp. is in Clade V and is the first microsporidium isolated from a crayfish with genetic data placing it in Clade V. Knowledge of multiple microsporidian pathogens from across the phylogenetic tree of the Microsporidia hints of a diverse assemblage of microsporidian parasite origins in crayfish. For example, *Bacillidium* sp. PLFB32 (Dunn et al., 2009; Clade III) isolated via PCR from *Pacifastacus leniusculus* could possibly have been contracted from a protistan host, as many parasites in Clade III are known to infect protists. Alternatively, this isolate may have been amplified via PCR from an infected protist within or on the surface of the crayfish host. A further example includes *Nosema* (formerly *Vairimorpha*) *cheracis* and *Vairimorpha autopotamobii*, two microsporidian parasites from Clade I, but which are the only two identified from this Clade to infect Decapoda. Clade I primarily includes microsporidiens that infect insects, cladocerans and copepods (Vossbrinck et al., 2014); suggesting there may be a trophic link facilitating transmission between insect and crustacean hosts for this group. Finally, *Vittaforma* sp. PLDH3, a Clade IV microsporidium also isolated using PCR from *P. leniusculus* (Dunn et al., 2009), shows some similarity (91.28%) to described *Vittaforma corneae* (KP099339) isolated from human eye tissue, and Microsporidium sp. BLAT7 (FJ756054) (95.53% sim.) from *Brandtia latissima lata* (Amphipoda), suggesting that some

microsporidia that infect crayfish and other crustaceans have co-evolutionary links to those infecting other species, including humans.

In Claude V., *Vavraia parastacida* (isolated from *Cherax* sp.) and *Pleistophora soganderesi* (isolated from *Cambarellus puer*) are microsporidia described from crayfish, but lack SSU sequence data for comparison (Sogandares-Bernal, 1962; Sogandares-Bernal, 1965; Langdon, 1991a; Langdon, 1991b; Langdon and Thorne, 1992). It is unlikely that *Pleistophora soganderesi* is adequately described due to multiple morphological differences that are not accepted for the Pleistophoridae (Longshaw, 2011). *Pleistophora soganderesi*, described from a North American crayfish (*Cambarellus* sp.), has 19–21 turns of the polar filament and a relatively similar spore size and development process to *Cambaraspora floridanus* n. gen. n. sp., suggesting that the new genus *Cambaraspora* may be a more accurate placement for that parasite, which currently has no genetic data.

## 5.2. Taxonomy of the Glugeidae and inclusion of crustacean-infecting species

Species in the family Glugeidae are generally known to infect piscine hosts, have no intermediate hosts, and include no crustaceans in the host range (Thélohan, 1895). Until recently, microsporidia with > 80% genetic similarity to the Glugeidae had only been isolated from fish species in marine and freshwater environments (most recent description: Al Quraishi et al., 2019); however, a “*Pleistophora* sp.” 18S sequence isolate from a penaeid shrimp host (*Penaeus aztecus*) is deposited under GenBank accession number AJ252958 and is > 90% similar to a Glugeidae species, *Glugea hertwigi* (Cheney et al., 2000). The closest true *Pleistophora* sp. (*Pleistophora hippoglossoides*) to AJ252958 is 88% similar. Further, isolate AJ252958 shows only 11% similarity to *Trachipleistophora hominis* (Cheney et al., 2000) the human pathogen, suggesting that placement of this parasite infecting *P. aztecus* within the genus *Pleistophora* may need altering pending further study (Cheney et al., 2000). Such data suggest that aquatic hosts might be the source of Clade V microsporidian infections in humans (Cheney et al., 2000), and corroborates a similar hypothesis pertaining to the origins of human

infection by parasites from Clade IV Microsporidia in aquatic hosts (Tourtip et al., 2009; Bojko et al., 2017; Stentiford et al., 2019). Discovery of this microsporidium in *P. aztecus* was also the first account of a microsporidian parasite of a crustacean that falls within the Glugeidae using DNA sequence data. Our discovery of a novel microsporidian in a crayfish host is the second. *Glugoides intestinalis* from *Daphnia* sp., once suggested to be part of the Glugeidae, shows greater genetic similarity to the Vittaformia (Clade IV) (Larsson et al., 1996; Refardt et al., 2002).

*Cambaraspora floridanus* (and others in the complex) share less than 90% sequence similarity to all currently described microsporidian species. At the nucleotide level, the closest described species is *Glugea plegoclossi*, a parasite of multiple fish hosts (e.g. *Sardina pilchardus*, *Plecoglossus altivelis*). Based on our phylogenetic analyses, the new isolate branched alongside 'Microsporidium cypselurus' an informally described species from flying fish (*Cypselurus pinnatibarbus*) (Yokoyama et al., 2002). These associations suggest that *C. floridanus* has an evolutionary ancestor shared with some lineages of fish-infecting and crustacean-infecting Microsporidia. Fig. 8 shows that *C. floridanus* is a basal branching microsporidian to the genera: *Glugea*, *Heterosporis*, *Pseudoloma*, *Loma*, and *Ichthyosporidium*, which all exclusively infect fish.

In addition to the genetic similarity between *C. floridanus* and fish-infecting microsporidians from the Glugeidae, morphological similarities are also observed. The novel isolate develops in a sporophorous vesicle (pansporoblastic membrane) throughout its developmental cycle, as do members of *Loma*, *Pseudoloma*, *Heterosporis*, and *Ichthyosporidium* (Matthews et al., 2001; Azevedo and Matos, 2002; Sanders et al., 2012; Al Quraishi et al., 2019). Another morphological similarity is a relatively high number of polar filament coils, ranging from 13–16 through to 32–46 turns. Tissue tropism of *C. floridanus* in *P. paeninsularus* is restricted to muscle tissue; however, piscine tissues infected by the other genera in the Glugeidae include liver, nervous system, muscle, and epithelia among others, suggesting a limited tissue specificity in crustacean hosts.

Recent data published by Stentiford et al. (2018) provide evidence for trophic transfer of Clade V microsporidians between fish and crustacean hosts. Our phylogenetic data here, which highlight a crustacean-infecting microsporidium among fish-infecting microsporidia, suggests the same hypothesis. Future screening of fish from the Wacissa River in Florida for the presence of *C. floridanus* would help determine whether this microsporidian is trophically-transferred and present in other host taxa. Grayfish are an abundant and common prey item for many freshwater fishes, so considering the relatively high prevalence of *Cambaraspora floridanus* within the crayfish population, it is likely that fish are consuming infected crayfish. Future research will determine the effects of the parasite on both crayfish and fish populations in freshwater ecosystems.

### 5.3. Ecological impacts of invasive crayfish

Approximately 77% of the world's crayfish species occur in North America (Taylor et al., 2007). Exotic crayfish invasions in this region are a leading threat to native crayfish, and multiple crayfish species from both within and outside the continent have invaded new drainages (Taylor et al., 2007). *Procambarus paeninsularus* is a freshwater crayfish native to southern Georgia, extreme south-eastern Alabama, and much of central and northwestern Florida to the Choctawhatchee River Basin (Hobbs, 1981). *Procambarus paeninsularus* is in the subgenus *Scapulicambarus* along with several other species, most notably *P. clarkii*, the red swamp crayfish (Hobbs, 1989). *Procambarus paeninsularus* is not known to be invasive, but *P. clarkii* has been introduced around the world via aquaculture, bait, and the pet trade, and it is invasive on every continent except Australia and Antarctica (Hobbs et al., 1989; Lodge et al., 2012). *Procambarus clarkii* is known to negatively affect native macrophytes, macroinvertebrates, fish and amphibians (Lodge et al., 2012; Twardochleb et al., 2013). Further, this species constructs

burrows, which can increase turbidity and nutrients that promote algal blooms and impact canals and water control structures (Yamamoto, 2010; Souty-Grosset et al., 2016). While it is unclear whether *C. floridanus* can infect *P. clarkii*, it could potentially be useful as a biocontrol agent, pending research on host range and susceptibility, as suggested previously for other parasites (Aquiloni et al., 2010; Häfpling et al., 2011; Lacey and Georgis, 2012).

### Acknowledgements

Thanks to Karen Kelly and Nicole Machi at the Electron Microscopy Core (University of Florida, Interdisciplinary Centre for Biotechnology Research) for their work on this pathogen and to Misty Penton, Emily An and Lucas Jennings for assistance with the collection of crayfish. Funding for this research was provided by the University of Florida.

### Appendix A. Supplementary material

Supplementary data to this article can be found online at <https://doi.org/10.1016/j.jip.2020.107345>.

### References

- Al Quraishi, S., Abdel-Gaber, R., El Deeb, N., Maher, S., Al-Shaebi, E., Abdel-Ghaffar, F., 2019. Ultrastructure and phylogenetic characterization of the microsporidian parasite *Heterosporis lessepsianus* n. sp. (Microsporidia: Glugeidae) infecting the lizardfish *Saurida lessepsianus* (Pisces: Synodontidae) inhabiting the Red Sea. *Microb. Pathog.* 130, 10–18.
- Aquiloni, L., Brusconi, S., Cecchinelli, E., Tricarico, E., Mazza, G., Paglanti, A., Gherardi, F., 2010. Biological control of invasive populations of crayfish: the European eel (*Anguilla anguilla*) as a predator of *Procambarus clarkii*. *Biol. Invasions* 12 (11), 3817–3824.
- Azevedo, C., Matos, E., 2002. Fine structure of a new species, *Loma myrophis* (Phylum Microsporidia), parasite of the Amazonian fish *Myrophis platyrhynchus* (Teleostei, Ophichthidae). *Eur. J. Protistol.* 37 (4), 445–452.
- Bacela-Spychalska, K., et al., 2018. Europe-wide reassessment of *Dictyocoela* (Microsporidia) infecting native and invasive amphipods (Crustacea): molecular versus ultrastructural traits. *Sci. Rep.* 8 (1), 8945.
- Baker, M.D., Vossbrinck, C.R., Maddox, J.V., Undeen, A.H., 1994. Phylogenetic relationships among *Vairimorphae* and *Nosema* species (Microspora) based on ribosomal RNA sequence data. *J. Invertebr. Pathol.* 30, 509–518.
- Balbiani, E., 1882. Sur les microsporidies ou psorospermes des articules. *Compt. Rend. Acad. Sci. Paris* 95, 1168–1171.
- Baquero, E., Rubio, M., Moura, I.N., Pieniazek, N.J., Jordana, R., 2005. *Myosporidium merluccius* n. sp. infecting muscle of commercial hake (*Merluccius* sp.) from fisheries near Namibia. *J. Eukaryot. Microbiol.* 52 (6), 476–483.
- Bojko, J., Clark, F., Bass, D., Dunn, A.M., Stewart-Clark, S., Stebbing, P.D., Stentiford, G.D., 2017. *Parahepatospora carcinii* n. gen., n. sp., a parasite of invasive *Carcinus maenas* with intermediate features of sporogony between the Enterocytozoon clade and other Microsporidia. *J. Invertebr. Pathol.* 143, 124–134.
- Bojko, J., Behringer, D.C., Moler, P., Reisinger, L., 2020. *Ovipleistophora diplostomuri*, a parasite of fish and their trematodes, also infects the crayfish *Procambarus bivittatus*. *J. Invertebr. Pathol.* 169, 107306.
- Cheney, S.A., Lafraanchi-Tristem, N.J., Canning, E.U., 2000. Phylogenetic relationships of Pleistophora-like microsporidia based on small subunit ribosomal DNA sequences and implications for the source of *Trachipleistophora hominis* infections. *J. Eukaryot. Microbiol.* 47 (3), 280–287.
- Doflein, F., 1901. Die Protozoen als Parasiten und Krankheitserreger nach biologischen Gesichtspunkten dargestellt. Fischer.
- Dunn, J.C., McClymont, H.E., Christmas, M., Dunn, A.M., 2009. Competition and parasitism in the native White Clawed Crayfish *Austropotamobius pallipes* and the invasive Signal Crayfish *Pacifastacus leniusculus* in the UK. *Biol. Invasions* 11 (2), 315–324.
- Gherardi, F., Aquiloni, L., Diéguez-Uribondo, J., Tricarico, E., 2011. Managing invasive crayfish: is there a hope? *Aquat. Sci.* 73 (2), 185–200.
- Häfpling, B., Edwards, F., Gherardi, F., 2011. Invasive alien Crustacea: dispersal, establishment, impact and control. *Biocontrol* 56 (4), 573–595.
- Hobbs Jr., H.H., 1981. The crayfishes of Georgia. *Smithsonian Contrib. Zool.* 318, 549.
- Hobbs, H.H., 1989. An illustrated checklist of the American crayfishes (Decapoda: Astacidae, Cambaridae, and Parastacidae). *Smithsonian Contrib. to Zool.* 480, 236.
- Hobbs, H.H., Jass, J.P., Huner, J.V., 1989. A review of global crayfish introductions with particular emphasis on two North American species (Decapoda, Cambaridae). *Crustaceana* 56, 299–316.
- Karpov, S., Mamkaeva, M.A., Aleoshin, V., Nassanova, E., Lilje, O., Gleason, F.H., 2014. Morphology, phylogeny, and ecology of the aphelinids (Aphelinidae, Opisthoskonta) and proposal for the new superfamily Opisthosporidia. *Front. Microbiol.* 5, 112.
- Lacey, L.A., Georgis, R., 2012. Entomopathogenic nematodes for control of insect pests above and below ground with comments on commercial production. *J. Nematol.* 44 (2), 218.

- Langdon, J.S., 1991a. Description of *Vavraia parastacida* sp. nov. (Microspora: Pleistophoridae) from marron, *Cherax tenuimanus* (Smith), (Decapoda: Parastacidae). *J. Fish Dis.* 14, 619–629.
- Langdon, J.S., 1991b. Microsporidiosis due to a pleistophorid in marron, *Cherax tenuimanus* (Smith), (Decapod: Parastacidae). *J. Fish Dis.* 14, 33–44.
- Langdon, J.S., Thorne, T., 1992. Experimental transmission per os of microsporidiosis due to *Vavraia parastacida* in the marron, *Cherax tenuimanus* (Smith), and yabby, *Cherax albifus*. *Clark J. Fish Dis.* 15, 315–322.
- Larsson, J.R., Ebert, D., Vávra, J., Voronin, V.N., 1996. Redescription of *Pleistophora intestinalis* Chatton, 1907, a microsporidian parasite of *Daphnia magna* and *Daphnia pulex*, with establishment of the new genus *Glugoides* (Microspora, Glugeidae). *Eur. J. Protistol.* 32 (2), 251–261.
- Lodge, D.M., et al., 2012. Global introductions of crayfishes: evaluating the impact of species invasions on ecosystem services. *Annu. Rev. Ecol. Evol. Syst.* 43, 449–472.
- Longshaw, M., 2011. Diseases of crayfish: a review. *J. Invertebr. Pathol.* 106, 54–70.
- Matthews, R.A., Matthews, B.F., 1980. Cell and tissue reactions of turbot *Scophthalmus maximus* (L.) to *Tetramicra brevifilum* gen. n., sp. n. (Microspora). *J. Fish Dis.* 3 (6), 495–515.
- Matthews, J.L., Brown, A.M., Larison, K., Bishop-Stewart, J.K., Rogers, P., Kent, M.L., 2001. *Pseudoloma neurophilia* ng, n. sp., a new microsporidium from the central nervous system of the zebrafish (*Danio rerio*). *J. Eukaryot. Microbiol.* 48 (2), 227–233.
- Moodie, E.G., Le Jambre, L.F., Katz, M.E., 2003. Ultrastructural characteristics and small subunit ribosomal DNA sequence of Vairimorpha cheracis sp. nov., (Microspora: Burenellidae), a parasite of the Australian yabby, *Cherax destructor* (Decapoda: Parastacidae). *J. Invertebr. Pathol.* 84 (3), 198–213.
- Muhire, B.M., Varsani, A., Martin, D.P., 2014. SDT: a virus classification tool based on pairwise sequence alignment and identity calculation. *PLoS One* 9 (9), e108277.
- Ovharenko, M.O., et al., 2010. *Cucumispora dikerogammari* n. gen. (Fungi: Microsporidia) infecting the invasive amphipod *Dikerogammarus villosus*: a potential emerging disease in European rivers. *Parasitology* 137, 191–204.
- Refardt, D., Canning, E., Mathis, S., Cheney, S., Lafranchi-Tristem, N., Ebert, D., 2002. Small subunit ribosomal DNA phylogeny of microsporidia that infect *Daphnia* (Crustacea: Cladocera). *Parasitology* 124, 381–389.
- Sanders, J., Myers, M.S., Tomanek, L., Cali, A., Takvorian, P.M., Kent, M.L., 2012. *Ichthyosporidium weissii* n. sp. (Microsporidia) infecting the arrow goby (*Clevelandia ios*). *J. Eukaryot. Microbiol.* 59 (3), 258–267.
- Sogandares-Bernal, F., 1962. Presumable microsporidiosis in the dwarf crayfishes *Cambarellus puer* Hobbs and *C. shufeldti* (Faxon) in Louisiana. *J. Parasitol.* 48, 493.
- Sogandares-Bernal, F., 1965. Parasites from Louisiana crayfishes. *Tulane Stud. Zool.* 12, 79–85.
- Souto-Grosset, C., Anastácio, P.M., Aquiloni, L., Banha, F., Choquer, J., Chucholl, C., Tricarico, E., 2016. The red swamp crayfish *Procambarus clarkii* in Europe: impacts on aquatic ecosystems and human well-being. *Limnologica* 58, 78–93.
- Stentiford, G.D., Bateman, K.S., Small, H.J., Moss, J., Shields, J.D., Reece, K.S., Tuck, I., 2010. *Myospora metanephrops* (ng, n. sp.) from marine lobsters and a proposal for erection of a new order and family (Crustaceacida; Myosporidae) in the Class Marinospordia (Phylum Microsporidia). *Int. J. Parasitol.* 40 (12), 1433–1446.
- Stentiford, G.D., Feist, S.W., Stone, D.M., Bateman, K.S., Dunn, A.M., 2013. Microsporidia: diverse, dynamic, and emergent pathogens in aquatic systems. *Trends Parasitol.* 29 (11), 567–578.
- Stentiford, G.D., et al., 2016. Microsporidia—emergent pathogens in the global food chain. *Trends Parasitol.* 32 (4), 336–348.
- Stentiford, G.D., et al., 2018. Evidence for trophic transfer of *Inodosporus octospora* and *Ovipleistophora arlo* n. sp. (Microsporidia) between crustacean and fish hosts. *Parasitology* 145 (8), 1105–1117.
- Pretto, T., Montesi, F., Ghia, D., Berton, V., Abbadi, M., Gastaldelli, M., Fea, G., 2018. Ultrastructural and molecular characterization of Vairimorpha austropotamobii sp. nov. (Microsporidia: Burenellidae) and Thelohania contejeani (Microsporidia: Thelohaniidae), two parasites of the white-clawed crayfish, *Austropotamobius pallipes* complex (Decapoda: Astacidae). *J. Invertebr. Pathol.* 151, 59–75.
- Stentiford, G.D., Bass, D., Williams, B.A., 2019. Ultimate opportunists—the emergent Enterocytozoon group microsporidia. *PLoS Pathog.* 15 (5).
- Taylor, C.A., et al., 2007. A Reassessment of the conservation status of crayfishes of the United States and Canada after 10+ years of increased awareness. *Fisheries* 32 (8), 372–389.
- Thélohan, P., 1895. Recherches sur les Myxosporidies. *Bulletin Scientifique De la France et de la Belgique* 26, 100–394.
- Tourtip, S., et al., 2009. *Enterocytozoon hepatopenaei* sp. nov. (Microsporidia: Enterocytozoonidae), a parasite of the black tiger shrimp *Penaeus monodon* (Decapoda: Penaeidae): fine structure and phylogenetic relationships. *J. Invertebr. Pathol.* 102 (1), 21–29.
- Trifinopoulos, J., Nguyen, L.-T., von Haeseler, A., Minh, B.Q., 2016. W-IQ-TREE: a fast online phylogenetic tool for maximum likelihood analysis. *Nucleic Acids Res.* 44 (1), 232–235.
- Twardochleb, L.A., Olden, J.D., Larson, E.R., 2013. A global meta-analysis of the ecological impacts of nonnative crayfish. *Freshwater Sci.* 32, 1367–1382.
- Vossbrinck, C.R., Debrunner-Vossbrinck, B.A., Weiss, L.M., 2014. Phylogeny of the Microsporidia. Pathogens of Opportunity, Microsporidia, pp. 203–220.
- Weissenberg, R., 1976. Microsporidian interactions with the host cell. Comparative Pathobiology. Plenum Press, New York.
- Yamamoto, Y., 2010. Contribution of bioturbation by the red swamp crayfish *Procambarus clarkii* to the recruitment of bloom-forming cyanobacteria from sediment. *J. Limnol.* 69, 102–111.
- Yokoyama, H., Lee, S.J., Bell, A.S., 2002. Occurrence of a new microsporidium in the skeletal muscle of the flying fish *Cypselurus pinnatibarbus japonicus* (Exocoetidae) from Yakushima, Japan. *Folia Parasitologica* 49 (1), 9–15.